Water Research 108 (2017) 124–136

Contents lists available at ScienceDirect

Water Research

journal homepage: www.elsevier.com/locate/watres

Characterizing and contrasting the microbial ecology of laboratory and full-scale EBPR systems cultured on synthetic and real wastewaters

Erik R. Coats [a, *], Cynthia K. Brinkman [a], Stephen Lee [b]

[a] Department of Civil Engineering, University of Idaho, Moscow, ID 83844-1022, USA
[b] Department of Statistics, University of Idaho, Moscow, ID 83844-1104, USA

ARTICLE INFO

Article history:
Received 15 June 2016
Received in revised form
25 October 2016
Accepted 26 October 2016
Available online 28 October 2016

Keywords:
Illumina MiSeq
Enhanced biological phosphorus removal, EBPR
qPCR
Volatile fatty acids, VFAs
Crude glycerol
Phosphorus accumulating organisms, PAOs
Accumulibacter

ABSTRACT

The anthropogenic discharge of phosphorus (P) into surface waters can induce the proliferation of cyanobacteria and algae, which can negatively impact water quality. Enhanced biological P removal (EBPR) is an engineered process that can be employed to efficiently remove significant quantities of P from wastewater. Within this engineered system, the mixed microbial consortium (MMC) becomes enriched with polyphosphate accumulating organisms (PAOs). To date much knowledge has been developed on PAOs, and the EBPR process is generally well understood; nonetheless, the engineered process remains underutilized. In this study, investigations were conducted using qPCR and Illumina MiSeq to assess the impacts of wastewater (synthetic vs. real) on EBPR microbial ecology. While a strong relationship was demonstrated between EBPR metrics (P:C; influent VFA:P) and excellent P removal across diverse EBPR systems and MMCs, no such correlations existed with the specific MMCs. Moreover, MMCs exhibited distinct clusters based on substrate, and qPCR results based on the putative PAO Accumulibacter did not correlate with BLASTN eubacterial results for either Accumulibacter or *Rhodocyclaceae*. More critically, PAO-based sequences aligned poorly with Accumulibacter for both eubacterial and PAO primer sets, which strongly suggests that the conventional PAO primers applied in FISH and qPCR analysis do not sufficiently target the putative PAO Accumulibacter. In particular, negligible alignment was observed for PAO amplicons obtained from a MMC performing excellent EBPR on crude glycerol (an atypical substrate). A synthetic wastewater-based MMC exhibited the best observed BLASTN match of the PAO amplicons, raising concerns about the potential relevance in using synthetic substrates in the study of EBPR.

1. Introduction

The anthropogenic discharge of excess nutrients (specifically nitrogen, N, and phosphorus, P) into surface waters is being increasingly scrutinized for its adverse impact on water quality. Among the concerns is the proliferation of cyanobacteria and algae. Commonly attributed to excess P, *Cyanobacteria* outbreaks represent a serious health concern due to the production of cyanotoxins (Brooks et al., 2016; Paerl, 2014), which can be fatal to humans and animals if ingested. Examples of *Cyanobacteria* blooms are numerous. In 2014, drinking water service was cut to Oregon, Ohio (500,000 + customers) due to cyanotoxins in Lake Erie. More local to the authors, similar issues occur annually in the Spokane River (Washington), a popular recreational water body. In addition to the cyanotoxin concern, excess nutrients in aquatic environments (P in particular (Heathwaite and Sharpley, 1999)) leads to advanced surface water body eutrophication, which, in turn, can incur significant ecological and social damage (Pretty et al., 2003).

In an effort to reduce point-source P discharges, water resource recovery facilities (WRRFs) are facing increasingly stringent permit limitations. Enhanced biological P removal (EBPR) is an engineered WRRF process configuration that can be employed to achieve low effluent P concentrations. Compared to chemical treatment alternatives, EBPR is more environmentally sustainable (Coats et al., 2011c) and should be considered as a first line of defense in achieving wastewater P removal. Theoretically, successful EBPR requires repeatedly exposing a mixed microbial consortium (MMC) to an anaerobic environment in the presence of volatile fatty acids (VFAs) followed by an aerobic environment. Within this engineered system, the MMC becomes enriched with polyphosphate

* Corresponding author.
E-mail address: ecoats@uidaho.edu (E.R. Coats).

http://dx.doi.org/10.1016/j.watres.2016.10.069
0043-1354/

accumulating organisms (PAOs), which are the putative organisms responsible for EBPR. PAOs uptake and store VFAs anaerobically as polyhydroxyalkanoate (PHA); reducing equivalents for PHA synthesis are primarily provided by the catabolism of glycogen, while the ATP required for VFA uptake and activation is supplied by glycogen catabolism and polyphosphate (polyP) hydrolysis (Lemos et al., 2003; Seviour et al., 2003). These anaerobic metabolisms result in an increase in bulk solution P. In the subsequent aerobic environment, PAOs oxidize the stored PHA, which supplies the carbon and energy for growth and the recovery of internal glycogen and polyP reserves. Through this cyclical process, more P is stored than was released, resulting in the net removal of P.

To advance EBPR process knowledge, research has sought to identify the microorganisms constituting PAOs. Current knowledge on PAO microbiology is derived from the pioneering work by Bond et al. (1995, 1999) and Hesselmann et al. (1999). Investigating the process at the lab-scale and with synthetic wastewater, the former research team identified *Betaproteobacteria* within the *Rhodocyclus* group (an unofficial taxonomic classification containing *Rhodocyclus*, *Azoarcus*, and *Zoogloea* genera) enriched in EBPR systems. Subsequent investigations (Bond et al., 1999), applying fluorescence in-situ hybridization (FISH) using 16S and 23S rDNA oligonucleotide probes, confirmed the predominance of the *Betaproteobacteria* in EBPR systems while also identifying other bacteria within the same class that were synthesizing PHA, but not removing P. It was concluded that the non-EBPR bacteria were glycogen accumulating organisms (GAOs) that theoretically compete with PAOs in EBPR environments. Taking the MMC characterization further, Hesselmann et al. (1999), through a combination of 16S rDNA clone library analysis, polyP and PHA staining, and dot blot hybridization, identified a unique bacterial species consistent with the PAO phenotype. While genetically similar to *Rhodocyclus*, the identified bacterium did not exhibit the ability to grow phototrophically and was named *Candidatus* Accumulibacter phosphatis (henceforth referred to as Accumulibacter); Crocetti et al. (2000) drew similar conclusions. More recently, exploring the EBPR MMC based on inocula from Madison, WI (USA) and Queensland, Australia, Garcia Martin et al. (2006) published the first metagenome of an Accumulibacter-enriched MMC, and affirmed that this organism is related to *Rhodocyclus* (also noting it should be classified as its own genus).

Based on the work of Bond et al. (1995, 1999); Hesselmann et al. (1999), and Garcia Martin et al. (2006), Accumulibacter is broadly recognized as the model PAO (Oehmen et al., 2007). Indeed, most EBPR microbial ecology research has focused on examining and quantifying the relative abundance of Accumulibacter in EBPR MMCs, with a particular emphasis on applying 16S rDNA-based FISH (e.g., (Albertsen et al., 2012; Nielsen et al., 2010; Oehmen et al., 2007)) and, to a lesser degree, qPCR (e.g., (Coats et al., 2015; He et al., 2007; Mao et al., 2015; Winkler et al., 2011)). These 16S rDNA-based investigations leveraged oligonucleotide probes targeting Accumulibacter from Crocetti et al. (2000), wherein the putative PAO-specific probes were developed based on DNA recovered from three synthetic wastewater fed lab-scale EBPR MMC. However, the PAO phenotype has been observed in other distinct taxonomic groups, including *Tetrasphaera* (Nguyen et al., 2011), *Candidatus* Halomonas phosphatis (Nguyen et al., 2012) and *Gemmatimonas aurantiaca* (Zhang et al., 2003). Potentially confounding the apparent uncertainty in affirming what microorganisms constitute PAOs are i) the target-specific molecular methods (i.e., targeting Accumulibacter), which induces potential bias, ii) the source of MMCs examined in microbial ecology studies, and iii) the associated substrate on which the MMC were cultured. Most EBPR microbial ecology research has focused at the laboratory scale and commonly with synthetic wastewater; such approaches deviate from the full-scale environments to which this WRRF technology is applied. While next generation sequencing methods (e.g., 454 pyrosequencing and Illumina MiSeq) have been applied in a limited manner to more broadly characterize microbial communities in pilot or full-scale WRRFs, some of which were EBPR systems (Hu et al., 2012; Kim et al., 2013; Liu et al., 2016; Wang et al., 2012; Wen et al., 2015), in all cases the focus was more on describing the MMC and less on understanding the MMC within the context of EBPR.

While over the past 25 years substantial gains have been realized in understanding the EBPR process at a macro- and micro-level, nonetheless the process remains underutilized at full-scale largely due to concerns over process stability and reliability (Oehmen et al., 2007). From a microbiological perspective, considering the relative diversity of putative PAOs observed in EBPR studies (including, but not exclusively, Accumulibacter), the importance of any given species or particular enrichment is in question; indeed, the collective body of EBPR microbiological research suggests induced function of a diverse PAO enrichment is perhaps more critical in realizing overall process success. However, in pursuit of an enhanced perspective on MMC structure vs. induced function, there is a dearth of research contrasting important parameters: operational scale and substrate (i.e., real vs. synthetic). Our research group has extensively investigated the EBPR process (Al-Najjar et al., 2011; Coats et al. 2011a, 2011b, 2011c, 2015; Horgan et al., 2010; Winkler et al., 2011), with a particular emphasis on expanding process knowledge and understanding through the predominant use of real wastewater. Recent research demonstrated the successful use of crude glycerol (an atypical EBPR substrate) in accomplishing excess P removal (Coats et al., 2015). Moreover, investigations have collectively revealed variable PAO fractions in EBPR MMCs (lab- and full-scale systems; applying qPCR based on Accumulibacter primers) seemingly independent of substrate and process performance. Building upon these past investigations, research was conducted to characterize EBPR performance and associated MMCs enriched under differing substrate conditions and in lab-versus full-scale EBPR systems, with a particular emphasis on generating new insight on the structure-function relationship. In executing this research, we posited:

(1) PAO research has largely centered on Accumulibacter, with methods for quantification including FISH and qPCR using primers specific for Accumulibacter. However, the 16S rDNA PAO results have not been interrogated beyond FISH and qPCR. Herein we consider Next Gen Sequencing results related to EBPR MMC, applying both eubacterial and PAO primer sets; results are evaluated based on phylotype classification.
(2) %PAO in a MMC is not correlated with P removal (or any EBPR process metrics). Research to date has yet to yield a convincing causal relationship, apart from the fact that PAOs must be present. In other words, once a PAO population is are established, induced metabolisms dictate process outcomes, and the %PAOs themselves are not indicative of the success of the process in general.
(3) Unique, potentially distinct communities are selected for lab- and full-scale systems. Additionally, the MMC enriched by synthetic substrates are distinct from those enriched by real wastewater.

2. Materials and methods

2.1. Operating conditions and system assessments

Four laboratory-scale EBPR sequencing batch reactors (SBRs)

and one full-scale WRRF system (the Moscow, ID WRRF; an A^2/O EBPR process) were evaluated. The SBRs were differentiated by substrate: R-EBPR received only raw wastewater, V-EBPR received a traditional EBPR substrate of raw wastewater and VFA-rich fermenter liquor, G-EBPR received raw wastewater and crude glycerol, and S-EBPR received a synthetic substrate. Each SBR was operated with a 6 h cycle consisting of the following periods: feed (5 min), anaerobic (1 h), aerobic (4.25 h), settle (30 min), and decant (10 min). A programmable logic controller was used to maintain SBR operations. SBRs were operated at 2 L (maximum volume during the cycle) with effluent decanted during each cycle and replaced with an equal volume of substrate to maintain an 18 h hydraulic residence time (HRT). The solids residence time (SRT) was controlled at 10 d by automatically wasting 50 mL of mixed liquor per cycle at the end of each aerobic period prior to settling. Air was introduced through stone diffusors to create aerobic conditions (dissolved oxygen (DO) > 2 mg L^{-1}) for the first 3.75 h of the aerobic period. The remainder of the aerobic period proceeded without aeration to allow depletion of residual DO and ensure that anaerobic conditions prevailed at the beginning of the subsequent cycle. Occasional DO checks throughout the operational cycle were used to confirm each SBR conformed to target DO concentrations (data not shown). Reactors were mixed with magnetic stir bars and operated at room temperature without pH control. All pumping was performed using peristaltic pumps (Watson Marlow, Wilmington, MA, USA). R-, V-, and G-EBPR have been the subjects in previous work (Coats et al., 2015); however, the data presented herein is unique to this study.

The Moscow WRRF services a community of approximately 25,000 people with an average influent flow rate of approximately 11,400 m^3 d^{-1} (predominantly domestic wastewater). The system consists of three anaerobic basins (each 787 m^3), two pre-anoxic basins (each 1363 m^3), an aerobic oxidation ditch (6814 m^3), and two 7570 m^3 secondary clarifiers, with influent wastewater pretreated through a 6 mm perforated plate screen followed by a vortex grit basin. The WRRF operates at a total SRT of 15–18 d. The return activated sludge flow rate is fixed at 4088 m^3 d^{-1}, while the aerobic basin mixed liquor return flow rate to the first pre-anoxic basin is controlled using a nitrate probe in the second pre-anoxic basin (target anoxic effluent NO_3–N of 0.5–1.0 mg L^{-1}).

The SBR and Moscow WRRF systems were each characterized on seven operational days (with 5 October 2014 being operational day zero, the date on which S-EBPR was considered at steady-state). System assessments took place on operational days 72, 86, 107, 121, 241, 263, and 283 for the four SBRs and on operational days 225, 255, 270, 284, 304, 313, and 320 for the Moscow WRRF.

2.2. Source of microorganisms, wastewater, and crude glycerol

SBR inocula were obtained from the Moscow WRRF. Each reactor was inoculated independently; however, on operational day 147 S-and G-EBPR experienced a process upset due to excess reactor wasting. G-EBPR was immediately re-inoculated from V-EBPR, while S-EBPR was allowed to recover independently. Thereafter, SBR system assessments were postponed for 93 d to reestablish steady-state.

Raw wastewater was obtained from the Moscow WRRF, downstream of screening and grit removal. VFA-rich fermenter liquor was recovered from a bench-top fermenter fed thickened primary solids from the Pullman, WA WRRF (Coats et al., 2011a). Crude glycerol (CG) was acquired from the pilot-scale biodiesel production system operated by the Biological and Agricultural Engineering Department at the University of Idaho (Moscow, ID, USA) (Thompson and He, 2006). CG was fed separately to the G-EBPR reactor, with a bulk solution CG concentration (t = 0) of approximately 1.0 Cmmol L^{-1}. Fresh raw wastewater was obtained every 2–7 d, filtered through a 53 μm stainless steel sieve (Gilson Company, Inc., Lewis Center, OH, USA), and stored at 4 °C until use. Bioreactor substrate tanks were replenished daily. The unsterilized synthetic substrate for the S-EBPR reactor (based on Lu et al. (2006)) consisted of (concentrations in the total feed volume prior to reactor addition): $NaCH_3COOH$ (281 mg L^{-1}); CH_3CH_2COOH (173 mg L^{-1}); NH_4Cl (60.1 mg L^{-1}); $CaCl_2$–H_2O (11.7 mg L^{-1}); K_2HPO_4 (8.4 mg L^{-1}); KH_2PO_4 (8.4 mg L^{-1}); $MgSO_4$–$7H_2$ (52.8 mg L^{-1}); peptone (2.2 mg L^{-1}); and yeast extract (2.2 mg L^{-1}). Trace nutrients were added as per Lu et al. (2006). Nitrification was inhibited through the combined addition of thiourea (15 mL (V-EBPR), 35 mL (G- and R-EBPR); stock concentration 40 g L^{-1}) and nitrapyrin ($ClC_5H_3NCCl_3$; 1–2 mL (V-EBPR), 1.5–2 mL (G- and R-EBPR); stock concentration 0.5% in 95% EtOH) into the daily total substrate volume. Nitrapyrin was added because thiourea proved to be only partially capable of inhibiting nitrification. Nitrate was periodically measured to confirm nitrification was indeed inhibited.

2.3. Analytical techniques

Samples were monitored for soluble reactive phosphate (SRP), volatile fatty acids (VFAs), nitrate (NO_3), mixed-liquor suspended solids (MLSS), glycogen, PHA, and glycerol as described in Coats et al. (2015). Measurement of pH was accomplished with a Thermo-Fisher Scientific Accumet AP85 Waterproof pH/Conductivity Meter. DO measurements were collected using a Hach HQ30d Meter with a LDO101 DO Probe.

2.4. Quantitative polymerase chain reaction (qPCR)

qPCR was performed on genomic DNA recovered during each system assessment to estimate the abundance of Accumulibacter (the model PAO) and glycogen accumulation organisms (GAOs) relative to the total eubacterial population. Genomic DNA was extracted using the MO BIO PowerSoil® DNA Isolation Kit (MO BIO Laboratories Inc., Carlsbad, CA USA). Genomic DNA yield and purity was quantified using a Synergy H1 Multi-Mode Reader (BioTek, Winooski, VT). Primer sets used to quantify total bacteria (Muyzer et al., 1993), Accumulibacter (Crocetti et al., 2000; He et al., 2007), and GAOs (by targeting *Candidatus* Competitbacter phosphatis, a model GAO) (Crocetti et al., 2002) are listed in Table S4 qPCR settings were in accordance with Winkler et al. (2011). Triplicate qPCR was performed for all SBR samples both on a given 96 well plate (three replicate samples per plate) and on three plates (thus 9 replicates per SBR sample). qPCR (triplicate on a 96 well plate; n = 3) was applied to DNA extracted from the Moscow WRRF to align lab-scale operations with full-scale systems. qPCR melting curves were evaluated to confirm a single melting peak, and agarose gel analysis confirmed a single band for each primer set. Amplification efficiencies were calculated for each primer set using baseline-corrected fluorescence data (StepOne software v2.0) and the LinRegPCR program (Ramakers et al., 2003). Mean amplification efficiencies for the total bacterial, PAO, and GAO primer sets were 95.6 ± 0.085% (n = 254), 89.7 ± 0.088% (n = 250), and 82.3± 0.074% (n = 249) respectively. The cycle threshold was set at a constant value of 0.5 within the log-linear region across all samples for determination of quantification cycle (Cq) values. PAO and GAO relative abundances were estimated per Winkler et al. (2011).

2.5. DNA sequence analysis and taxonomic classification

Illumina sequencing was performed on genomic DNA recovered during each system assessment. Bacterial 16S rRNA gene fragments

were amplified and sequenced in accordance with Hanson et al. (2016a). DNA amplicons were generated using two PCR rounds (round one amplified the targeted region of the 16S rRNA gene and round two attached sequencing adapters and sample barcodes) for eubacteria (Shen et al., 2016), PAOs (Crocetti et al., 2000; He et al., 2007), and GAOs (Crocetti et al., 2002); the primers are described in Table S6. The barcoded amplicons were sequenced using an Illumina MiSeq instrument creating paired end 2 × 300 bp libraries (Illumina, Inc., San Diego, CA).

Sequence analysis and taxonomic classification were performed following Hanson et al. (2016a). Briefly, the Illumina MiSeq reads were demultiplexed and assigned to expected barcode and primer sequences using the Python script dbcAmplicons (https://github.com/msettles/dbcAmplicons). After the primer sequences were trimmed, the reads were joined into a single amplicon sequence using the application FLASH (Magoč and Salzberg, 2011). The Ribosomal Database Project (RDP) Naïve Bayesian classifier was then used to assign the joined sequences to phylotypes (Wang et al., 2007); assignment was made to the lowest taxonomic rank with a bootstrap score ≥50%. The relative abundance of individual phylotypes in each sample was determined as the percentage of the corresponding sequence reads among the total sequence reads in the sample.

As the RDP method is unable to identify Accumulibacter (Mao et al., 2015), an alternative method was used to estimate its relative abundance. First, 27 16S rRNA gene sequences were identified from He et al. (2007) as representatives of the 16S rRNA clades of Accumulibacter (following Mao et al. (2015); summarized in Table S136). These reference sequences were then classified with the RDP Bayesian classifier with a confidence threshold of 90%. While Accumulibacter has not been formally categorized, RDP classified all of the reference sequences as belonging to the *Rhodocyclaceae* family (Table S136). Expecting the same classification for Accumulibacter-related sequences in the samples, the subset of the joined sequences in each sample classified as belonging to *Rhodocyclaceae* by RDP was identified using BLASTN (v. 2.3.0+) (Camacho et al., 2009) from a database consisting of the 27 Accumulibacter reference sequences and the 16S rRNA gene sequences from the NCBI Nucleotides database assigned to *Rhodocyclaceae*. Sequences were assigned to Accumulibacter if the top BLASTN result was one of the 27 Accumulibacter reference sequences with at least 97% sequence similarity.

2.6. Data analysis

Custom software (altvisngs; available at https://github.com/nguho/altvisngs) was used to quantify the sample diversity and evenness indices, complete the rarefaction and hierarchical cluster analysis, and generate the taxon hierarchy with relative abundance, heatmap, and summary bar plot images. Principal component analysis (PCA) was performed using R v3.2.5 (http://www.r-project.org/).

3. Results and discussion

3.1. Overall EBPR performance

The influent and effluent P of each SBR were monitored regularly throughout the operational period, with S-, V-, and G-EBPR achieving 95% or greater P removal on average (Table 1; Fig. S1). Consistent with our previous study (Coats et al., 2015), R-EBPR was less effective in accomplishing P removal, achieving only 49% P removal on average. Of the four SBRs, G-EBPR most consistently achieved effluent P below 1 mg P L^{-1} over the operational period (Fig. S1C). Even with several minor process upsets (Table 2), effluent P from S-EBPR and V-EBPR was also less than 1 mg P L^{-1} for most of the operational period (Fig. S1A and B). While R-EBPR exhibited effluent P comparable to the other three SBRs at times, such performance was ephemeral (Fig. S1D). Note that on operational days 268 and 269 the raw wastewater substrate was contaminated by an unknown antibacterial agent; this wastewater induced an upset in V-, G-, and R-EBPR, and was the only upset observed in G-EBPR over the operational period (effluent P > 3 mg P L^{-1}).

Regarding intra-cycle performance, as shown (Figs. S2–S5) the archetypal EBPR response was exhibited by the MMCs in S- and V-EBPR (anaerobic P release with subsequent aerobic P removal from bulk solution). In contrast, the MMCs in G- and R-EBPR did not consistently cycle P in accordance with EBPR theory. The lack of anaerobic P release by the G-EBPR MMC, coupled with its P removal in excess of 95%, has been examined and discussed in detail previously (Coats et al., 2015). All SBR MMCs consumed the available VFA substrate (and glycerol for G-EBPR) during the anaerobic period (data not shown, but consistent with the previous study), and commensurately synthesized PHA (Table S1) in accordance with EBPR theory. Also consistent with EBPR theory, glycogen was utilized anaerobically by all but R-EBPR (Table S1).

3.2. EBPR process metrics

Two metrics are recognized as indicators of potential EBPR process success associated with a MMC enriched with PAOs: the anaerobic phosphorus released-to-VFA uptake (P:C) ratio (a characteristic of the PAO metabolic response (Filipe et al., 2001; Smolders et al., 1994)), and the ratio of influent organic substrate to total P removed (Grady et al., 2011). For the P:C ratio, consistent anaerobic P release was observed in both S- and V-EBPR (Figs. S2 and S3; Table 1), with average P:C ratios exceeding 0.19 P mol $Cmol^{-1}$ (total VFA basis). Conversely, G- and R-EBPR exhibited average P:C ratios of 0.04 and 0.06 P mol $Cmol^{-1}$. The G-EBPR MMC did not always realize anaerobic P release (consistent with and as discussed in Coats et al. (2015)), nor did the R-EBPR MMC (Figs. S4 and S5). Data from this and previous studies (Coats et al., 2011a, 2011b, 2015; Horgan et al., 2010; Winkler et al., 2011) were coupled with unpublished data obtained from our pilot-scale EBPR system (1:1000 scale of the Moscow WRRF) to examine the potential relationship of P:C with effluent P. As shown (Fig. 1), there appears to be a relationship between P:C and effluent P; excepting the S-EBPR data points, P:C ratios exceeding 0.2 resulted in effluent SRP less than 0.5 mg L^{-1}. According to Lopez-Vazquez et al. (2007), and as summarized in Oehmen et al. (2007), such P:C ratios would appear to favor the enrichment of PAOs over GAOs, although the ratios were lower than would be predicted by the model of Filipe et al. (2001).

Regarding the ratio of influent organic substrate to total P removed, the premise is that a minimum amount of organic carbon (preferably VFAs) is necessary to realize the target PAO enrichment capable of performing EBPR. The organic substrate is typically expressed on a biochemical oxygen demand (BOD) or chemical oxygen demand (COD). Research indicates a relationship between influent BOD and total P removed, with suggested minimum values ranging from 15 to 20 BOD:P and 26-34 COD:P for high efficiency EBPR (summarized in (Grady et al., 2011; WEF, 2010)). While BOD and COD are measurements that can readily be tested at full-scale WRRFs, both are gross aggregates of potential carbon substrate that do not specifically identify the organic carbon substrate driving EBPR (VFAs). Coupling this study with previous research (Coats et al., 2011a, 2011b; Horgan et al., 2010; Winkler et al., 2011) and unpublished pilot- and full-scale operational data, results compiled in Fig. 2 indicate an influent ratio of 15 mg VFA (as COD) per mg P

Table 1
Performance characteristics for each SBR and Moscow WRRF, by operational day, including influent/effluent phosphorus and % P removal. Influent wastewater VFA:P ratio, phosphorus released anaerobically, and the anaerobic P:C ratio summarized for the SBRs.

	Op'l day	Infl. P, (mg L^{-1})	Effl. P, (mg L^{-1})	% P Removal	Infl. VFA:P (mg COD mg P^{-1})	P_{rel} (mg L^{-1})	P:C (P mol C mol^{-1})
S-EBPR	72	15.14	0.25	98.3	39.9	87.9	0.512
	86	19.31	2.20	88.6	31.8	46.9	−0.149
	107	18.82	1.08	94.3	33.6	53	0.284
	121	21.54	1.86	91.4	18.5	54.5	0.467
	241	16.48	0.35	97.9	30.2	69.1	0.469
	263	17.83	0.30	98.3	33.0	92.3	0.526
	283	21.31	0.44	97.9	20.0	85.2	0.679
V-EBPR	72	5.49	0.23	95.8	46.5	12.3	0.18
	86	6.17	0.03	99.5	30.3	9.4	0.172
	107	5.72	0.59	89.7	39.3	6.1	0.094
	121	6.59	0.10	98.5	33.2	8	0.13
	241	8.83	0.12	98.6	14.4	15.6	0.423
	263	4.40	0.25	94.3	47.5	12	0.197
	283	5.73	0.54	90.6	17.4	13.5	0.452
G-EBPR	72	3.04	0.17	94.4	15.4	1.12	0.079
	86	3.43	0.04	98.8	0.0	−0.97	No VFAs
	107	2.58	0.23	91.1	13.1	0.82	0.08
	121	3.49	0.04	98.9	0.0	0.55	no VFAs
	241	4.50	0.44	90.2	14.0	−0.31	−0.02
	263	3.22	0.13	95.7	24.1	1.18	0.05
	283	4.86	0.41	91.6	5.6	1.36	0.181
R-EBPR	72	3.04	2.47	18.8	15.4	0.06	0.004
	86	3.45	2.67	22.6	0.0	0	no VFAs
	107	2.58	2.49	3.5	13.1	0.64	0.063
	121	3.45	1.96	43.2	0.0	1.02	no VFAs
	241	4.34	1.56	64.1	14.1	2.78	0.156
	263	2.91	0.68	76.6	29.0	6.24	0.243
	283	3.49	3.35	4.0	0.0	2.29	no VFAs
Moscow WRRF	225	5.01	0.15	97.0	–	–	–
	255	4.42	0.39	91.2	–	–	–
	270	4.76	0.20	95.9	–	–	–
	284	4.59	0.16	96.5	–	–	–
	304	4.70	<0.05	>98.9	–	–	–
	313	4.99	<0.05	>99.0	–	–	–
	320	5.71	<0.05	>99.1	–	–	–

will both enrich for PAOs and induce the metabolic responses necessary for EBPR. Both S-EBPR and V-EBPR exceeded the target ratio (Table 1; Fig. 2). Conversely, R-EBPR exhibited inconsistent influent VFA:P ratios (VFAs were commonly absent from the wastewater) and overall poor P removal. While the influent VFA:P ratios for G-EBPR were similar to R-EBPR, performance was sustained through the addition of crude glycerol (Coats et al., 2015). The VFA:P threshold suggested herein to achieve low effluent P concentrations (based dominantly on real wastewater-based operations), being lower compared with guidance in Grady et al.

Table 2
Performance summary for the bench-scale EBPR reactors.

Parameter	Units	Reactor	Average	Maximum	Minimum	SD	n
MLSS	mg/L	S-EBPR	3888	6000	1530	1122	23
		V-EBPR	2631	3680	1740	632	23
		G-EBPR	2177	3040	780	598	18
		R-EBPR	1547	2500	900	435	12
Influent phosphorus	mgP/L	S-EBPR	18.11	27.80	12.98	3.08	63
		V-EBPR	5.68	8.24	3.76	0.98	64
		G-EBPR	4.13	5.32	2.51	0.85	28
		R-EBPR	3.97	5.51	2.34	0.95	28
Effluent phosphorus	mgP/L	S-EBPR	1.75[a]	47.87[a]	0.01	5.47	136
		V-EBPR	0.73[b]	7.06[b]	0.00	1.31	131
		G-EBPR	0.29[b]	3.59[c]	0.00	0.50	85
		R-EBPR	2.03	7.54	0.12	1.64	82
Influent VFA:influent P	mgVFA (as COD)/mgP	S-EBPR	31.85	43.95	19.66	7.53	14
		V-EBPR	33.34	49.23	15.47	11.34	11
		G-EBPR	12.35	29.32	0.00[d]	9.96	8
		R-EBPR	12.41	36.05	0.00[d]	12.46	8

[a] S-EBPR operations realized a temporary upset associated with misfeeding of synthetic substrate. Excluding approximately 30 days of operational instability, the maximum effluent S-EBPR phosphorus was 9.6 mg P/L, while the average was 0.68 mg P/L.
[b] Excluding 21 days that were deemed process upsets, the maximum effluent F-EBPR phosphorus was 0.92 mg P/L, while the average was 0.23 mg P/L.
[c] Excluding two observed days of process upset, the maximum effluent G-EBPR phosphorus was 0.54 mg P/L, while the average was 0.21 mg P/L.
[d] On several occasions both the G- and R-EBPR influent contained no VFAs, which is consistent with previous observations (Coats et al., 2015.

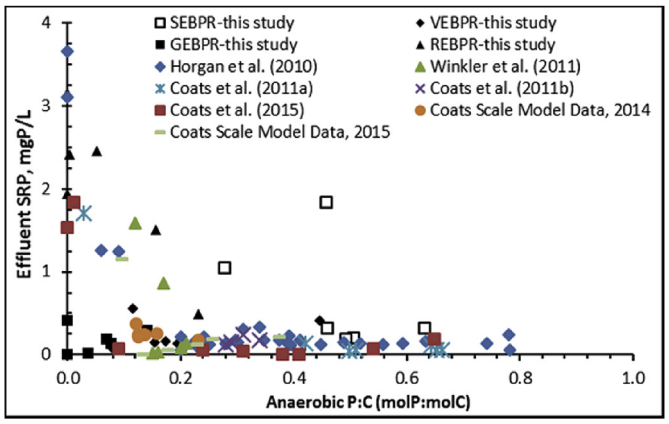

Fig. 1. Influent wastewater P:C ratio against effluent P for an array of laboratory-scale EBPR reactors (this study and (Coats et al., 2011a, 2011b, 2015; Horgan et al., 2010; Winkler et al., 2011)).

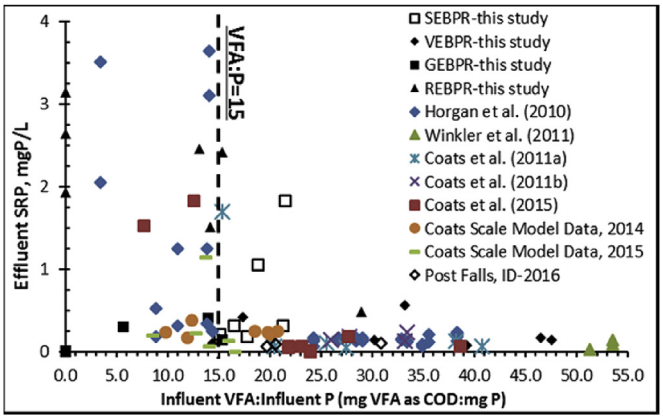

Fig. 2. Influent wastewater VFA:P ratio against effluent P for an array of laboratory-scale EBPR reactors (this study and (Coats et al., 2011a, 2011b, 2015; Horgan et al., 2010; Winkler et al., 2011)).

(2011) and the WEF Manual of Practice on Nutrient Removal (WEF, 2010), indicates that non-VFA substrates available in real wastewater also contributes to EBPR process stability and resiliency. Indeed, non-VFA substrate (e.g., glucose; glycerol (Coats et al., 2015)) can be used by microorganisms to directly generate energy (ATP) and PHA anaerobically in support of EBPR; the coupled P:C ratios presented herein, being low as contrasted with theoretical models (Filipe et al., 2001; Smolders et al., 1994), further support this observation (i.e., non-VFA substrate would not require polyP hydrolysis to generate energy for uptake and catabolism, thereby reducing the P:C ratio).

3.3. MMC characterization with qPCR

qPCR was applied to assess the abundance of PAOs and GAOs relative to the total eubacteria in the MMC (%PAO and %GAO, respectively) of each SBR and the Moscow WRRF during each of the seven system assessments. Considering methodological repeatability, the results were consistent within (triplicate) and across (triplicate) plates (i.e., low standard deviation; Table 3 and S3). The highest %PAO values were observed in S-EBPR and Moscow WRRF, with ranges of 0.61%–15.14% and 3.97%–17.54%, respectively. Comparatively, V-, G-, and R-EBPR exhibited markedly lower %PAO. Indeed, on all but one date (operational day 283) V-EBPR sustained %PAO less than 0.7% (range of 0.12–2.6%). Similarly, G-EBPR exhibited %PAO less than 0.82% (range of 0.26–0.82%), while R-EBPR (which, again, exhibited overall poor P removal) ranged from 0.11 to 1.14%. Collectively, the observed %PAO of the MMCs were generally consistent with our previous investigations for the V-, G-, and R-EBPR MMC (Coats et al., 2015), while lower than has been reported in other investigations (e.g., (He et al., 2007; Winkler et al., 2011)). Perhaps more critically, there was no relationship between EBPR performance and %PAO.

Also consistent with Coats et al. (2015), the %GAOs were generally low. The %GAO in S-EBPR was estimated at an order of magnitude lower than the %PAO (Table 3). However, the %GAO in the V-EBPR MMC was quantitatively comparable to, and at times higher than, the PAO fraction. GAOs were also present in the G-EBPR MMC, also approaching parity with %PAO. No GAOs were observed in the R-EBPR MMC (again consistent with Coats et al. (2015)). Comparatively, the %GAO in the Moscow WRRF was substantially lower than the %PAO (Table S3), and generally consistent with that observed in G-EBPR.

3.4. MMC characterization with next generation sequencing

3.4.1. Richness, rarefaction, and diversity analyses

Illumina sequencing targeting Eubacteria, PAOs, and GAOs was used to characterize the MMCs in the SBRs and the Moscow WRRF. The total number of joined sequences obtained for the Eubacteria primer set are summarized in Table S7 (similar data for PAO and GAO primer sets is summarized in Tables S50 and S93); detailed phylotype data can be referenced via Table S5. The number of reads for the Eubacteria primer set ranged from 1208 to 116,631; among the results there were two poor quality data sets (G-EBPR, day 283, 1208 reads; V-EBPR, day 263, 6428 reads). For Eubacteria, sequencing coverage depth was considered sufficient for each sample based on rarefaction analysis (Fig. S6 and S7). However, coverage for the PAOs and GAOs was insufficient for most, but not all, samples (Figs. S76, S77, S136, S137). In executing the experimental design for the MiSeq analysis, genomic DNA pooling for Eubacterial, PAO, and GAO analyses was based on prior qPCR results (Coats et al., 2015; Winkler et al., 2011). Ultimately, however, the analysis under-estimated the quantity of DNA needed to achieve full coverage for the PAO and GAO primer sets.

The Shannon index was calculated for the respective MMC to assess complexity. Three of the SBRs (V-, G-, and R-EBPR) exhibited similar complexity (average Shannon index of 3.90–3.94; range of 3.53–4.33; Table S7), while S-EBPR exhibited a slightly less complex microbial population (average Shannon index of 3.62; range of 3.36–3.9). In contrast, the Moscow WRRF MMC was the most complex (average Shannon index of 4.71). The Shannon index was selected for its value as a general complexity measure considering both richness and evenness (Hill et al., 2003). On the Shannon evenness scale, all SBR averages were similar while the Moscow WRRF again exhibited more complexity.

3.4.2. Eubacteria primer set

A comprehensive summary of the eubacterial-based MMC composition from the domain to genus level for each system assessment is presented in Figs. S14–S53 (see also Table S5). Table 4 summarizes the dominant phyla (averages across all operational days); the average microbial community composition in each SBR and the Moscow WRRF over the seven system assessments is presented in Figs. S21, S29, S37, S45, and S53. In all systems, *Proteobacteria* dominated the MMCs at the phylum level, followed by *Bacteroidetes*; no other phyla were, on average, observed at > 10%. In contrast, nine phyla predominated within the minor category (1–10%), and substantive differences were observed across the

Table 3
Results from qPCR applied to DNA extracted from MLSS obtained from each SBR and the Moscow WRRF. Data shown are composite averages/standard deviation for each operational day.

Op'l Day	S-EBPR		V-EBPR		G-EBPR		R-EBPR			Moscow WRRF	
	%PAO avg (SD)	%GAO avg (SD)	%PAO avg (SD)	%GAO avg (SD)	%PAO avg (SD)	%GAO avg (SD)	%PAO avg (SD)	%GAO avg (SD)	Op'l Day	%PAO avg (SD)	%GAO avg (SD)
72	4.17 (0.53)	0.21 (0.09)	0.67 (0.13)	0.45 (0.19)	0.40 (0.14)	0.05 (0.02)	0.52 (0.12	0.04 (0.03)	225	3.97 (0.11)	0.36 (0.01)
86	4.48 (0.63)	0.35 (0.17)	0.40 (0.07)	1.78 (0.63)	0.27 (0.03)	0.14 (0.07)	1.14 (0.27)	0.02 (0.01)	255	7.23 (0.30)	0.46 (0.03)
107	4.09 (1.19)	0.54 (0.34)	0.12 (0.03)	0.04 (0.02)	0.26 (0.06)	0.23 (0.11)	0.62 (0.14)	0.01 (0.01)	270	5.33 (0.59)	0.27 (0.02)
121	2.92 (1.37)	0.06 (0.02)	0.24 (0.12)	0.14 (0.03)	0.32 (0.07)	0.48 (0.23)	0.17 (0.05)	0.04 (0.03)	284	15.46 (0.46)	0.46 (0.05)
241	5.42 (2.21)	0.07 (0.03)	0.21 (0.08)	1.18 (0.61)	0.42 (0.17)	0.40 (0.19)	0.16 (0.04)	0.00 (0.00)	304	9.09 (0.79)	0.41 (0.02)
263	0.61 (0.11)	0.04 (0.02)	0.42 (0.15)	1.21 (0.58)	0.79 (0.29)	0.45 (1.32)	0.11 (0.05)	0.00 (0.00)	313	10.13 (0.49)	0.05 (0.00)
283	15.14 (3.70)	0.16 (0.04)	2.60 (0.54)	3.73 (0.64)	0.82 (0.23)	3.66 (1.32)	0.33 (0.09)	0.03 (0.01)	320	4.52 (0.10)	0.10 (0.01)

Table 4
Major and minor bacterial community composition at the phylum level (based on the calculated averages across all operational days evaluated; listed in order of dominance) detected for Eubacteria, PAOs, and GAOs in the lab- and full-scale EBPR WRRFs.

	S-EBPR	V-EBPR	G-EBPR	R-EBPR	Moscow
Eubacteria					
Major (>10%)	*Proteobacteria, Bacteroidetes*	*Proteobacteria, Bacteroidetes*	*Proteobacteria, Bacteroidetes*	*Proteobacteria, Bacteroidetes*	*Proteobacteria, Bacteroidetes*
Minor (>1%)	*Planctomycetes, Verrucomicrobia, Firmicutes, Chloroflexi*	*Verrucomicrobia, Actinobacteria, Firmicutes, Chloroflexi, Planctomycetes, Acidobacteria, Parcubacteria*	*Candidatus Saccharibacteria, Actinobacteria, Chloroflexi, Firmicutes, Verrucomicrobia*	*Verrucomicrobia, Plactomycetes, Chloroflexi, Actinobacteria, Acidobacteria, Firmicutes*	*Chloroflexi, Actinobacteria, Planctomycetes, Firmicutes, Candidatus Saccharibacteria, Verrucomicrobia, Acidobacteria, Nitrospirae*
PAOs					
Major (>10%)	*Proteobacteria*	*Proteobacteria,* Unknown bacterium, *Actinobacteria*	*Proteobacteria, Actinobacteria,* Unknown bacterium	*Proteobacteria*	*Proteobacteria,*
Minor (>1%)	–	*Chlamydiae*	*Verrucomicrobia, Chlamydiae*	Unknown bacterium, *Actinobacteria*	*Actinobacteria, Parcubacteria*
GAOs					
Major (>10%)	*Proteobacteria*	*Proteobacteria*	*Proteobacteria*	*Proteobacteria* Unknown bacterium	*Proteobacteria*
Minor (>1%)	Unknown bacterium	Unknown bacterium	Unknown bacterium	–	Unknown bacterium

MMC. Of the nine phyla, only V*errucomicrobia*, *Firmicutes*, and *Chloroflexi* were common to all MMCs; unique to the Moscow WRRF was *Nitrospirae*, a nitrifying phyla that would not have been expected in the SBRs due to the imposed nitrification inhibition. The Moscow WRRF MMC exhibited the largest number of minor phyla (9), while S-EBPR exhibited the fewest (4). Similar phylum-level analysis of the respective MMCs for the PAOs (Table 4; Figs. S84–S123; Table S5) again revealed that *Proteobacteria* dominated across the tested reactors, although *Actinobacteria* and an unknown *Bacteria* were observed at >10% in V- and G-EBPR; the PAO primer set targeted the *Proteobacteria* phyla. No minor phyla were observed in S-EBPR for the PAO primer set, while only 1-2 phyla were observed in the other four EBPR systems. For the GAO primer set, *Proteobacteria* dominated (except for R-EBPR, where an unknown *Bacteria* also predominated).

At the class level for the eubacterial primers, *Alphaproteobacteria* and *Betaproteobacteria* were the only two observed in the S-EBPR MMC at >10% (see Table S5; Figs. S14–S21). The V-, G-, and R-EBPR MMC, along with the Moscow WRRF, exhibited a similar composition, although *Betaproteobacteria* dominated over *Alphaproteobacteria*; *Sphingobacteria* was also observed at approximately 10%, but <4% in S-EBPR. Interrogating the MMCs at a lower rank (order; Table 5), the *Betaproteobacterium Rhodocyclales* and the *Alphaproteobacterium Rhodobacterales* were observed in S-EBPR at >10%; *Flavobacteriales*, from the *Bacteroidetes* phylum, was observed at nearly 10% of the total population as well. In contrast, *Hydrogenophilales*, from the *Betaproteobacteria* phylum, was more prominent in V- and R-EBPR, while *Sphingobacteriales* (of the *Bacteroidetes* phylum) was dominant in R-EBPR and also was the lone dominant order in the Moscow WRRF MMC. No dominant orders (>10%) were observed on average in G-EBPR across all operational days, although *Sphingobacteriales* averaged 9.87%. Note that the threshold for "minor" at the level of order was established at 5%, given the increased number of bacteria observed at >1%.

Finally, examining the MMC at the genus level, with the increased number of bacteria that can be identified, the threshold for "dominance" was adjusted to 3%. The S-EBPR MMC was predominated by (in order, highest to lowest) *Thauera*, *Flavobacterium*, *Ohtaekwangia*, and *Propionivibrio*. The V-EBPR MMC was predominated by *Thiobacillus*, *Haliscomenobacter*, *Thauera*, *Zoogloea*, and *Meganema* at the genus level, while G-EBPR was predominated by *Saccharibacteria_genera_inc._sed.*, *Haliscomenobacter*, *Methylobacillus*, *Zoogloea*, and *Meganema*. The R-EBPR MMC was enriched with three genera at >3% of the population (*Thiobacillus*, *Thauera*, and *Meganema*), while the Moscow WRRF only revealed one known genus at >3% (*Haliscomenobacter*).

The MiSeq results were also interrogated using multi-variate methods, which revealed interesting contrasts. First considering a Bray-Curtis similarity analysis, at the genus level all samples clustered by reactor (Fig. S13), with the exception of V-. G-, and R-EBPR (day 283) and V-EBPR (day 263). Both V-EBPR (day 263) and G-EBPR (day 283) exhibited low total reads (Table S7), which likely explains the associated result, and V-EBPR (day 263) exhibited low total reads relative to the other five sampled operational days. Considering the clustered results, the V- and G-EBPR MMC exhibited the closest similarity, followed by R-EBPR, the Moscow

Table 5
Major and minor bacterial community composition at the order level (based on the calculated averages across all operational days evaluated; listed in order of dominance) detected for Eubacteria, PAOs, and GAOs in the lab- and full-scale EBPR WRRFs.

	S-EBPR	V-EBPR	G-EBPR	R-EBPR	Moscow
Eubacteria					
Major (>10%)	*Rhodocyclales* *Rhodobacterales*	unknown *Bacteroidetes* *Hydrogenophilales*	–	*Hydrogenophilales* *Sphingobacteriales*	*Sphingobacteriales*
Minor (5–10%)	*Flavobacteriales* *Ohtaekwangia* *Rhizobiales* *Sphingobacteriales* *Planctomycetales* *Rhodospirillaes* *Burkholderiales* *Phycisphaerales* *Xanthomonadales* *Caulobacterales* *Verrucomicrobiales* *Myxococcales* *Sphingomonadales*	*Rhodocyclales* *Sphingobacteriales* *Burkholderiales* *Rhizobiales* *Cytophagales* *Bacteriodales* *Flavobacteriales* *Xanthomonadales* *Pseudomonadales* *Rhodobacterales* *Sphingomonadales* *Actinomycetales* *Rhodospirillales* *Clostridiales* *Caulobacterales* *Myxococcales* *Planctomycetales* *Caldilineales* *Parcubacteria*	*Sphingobacteriales* *Rhodocyclales* *Saccharibacteria* *Rhizobiales* *Hydrogenophilales* *Actinomycetales* *Burkholderiales* *Methylophilales* *Cytophagales* *Rhodobacterales* *Caulobacterales* *Flavobacteriales* *Ohtaekwangia* *Rhodospirillales* *Sphingomonadales* *Caldilineales* *Clostridiales* *Verrucomicrobiales* *Xanthomonadales* *Bdellovibrionales*	*Burkholderiales* *Rhizobiales* *Rhodocyclales* *Rhodobacterales* *Flavobacteriales* *Xanthomonadales* *Ohtaekwangia* *Planctomycetales* *Cytophagales* *Sphingomonadales* *Verrucomicrobiales* *Pseudomonadales* *Gp4*	*Flavobacteriales* *Burkholderiales* *Actinomycetales* *Rhodocyclales* *Rhizobiales* *Planctomycetales* *Chloroflexales* *Caldilineales* *Myxococcales* *Saccharibacteria* *Pseudomonadales* *Cytophagales* *Rhodobacterales* *Candidatus Carsonella* *Clostridiales* *Acidimicrobiales* *Rhodospirillales* *Ohtaekwangia* *Lactobacillales* *Phycisphaerales* *Xanthomonadales* *Nitrospirales*

WRRF, and lastly S-EBPR (i.e., synthetic wastewater-based MMC was distinctly different from all the real wastewater systems). Principal component analysis (PCA) confirmed these observations (Fig. 3; Figs. S66–S75). As shown (Fig. 3), the MMC at the genus level exhibited two distinct clusters within the first two PCA dimensions, with V-, G-, and R-EBPR uniquely separated from that of S-EBPR in both dimensions. Moreover, the 95% confidence region revealed much more variability within the real wastewater based MMC vs. S-EBPR. Combined, the first two dimensions explained 21.61% of the variation among the sample sets. When the Moscow WRRF samples were integrated into the analysis (Figs. S66–S75), while the comparative distinction at the genus level between V-, G-, and R-EBPR vs. S-EBPR remained, the relative separation becomes less pronounced while the Moscow MMC observations are quite uniquely separate (Fig. S74). For this second PCA, the first two dimensions explained 22.63% of the variation among the sample sets. In particular, the first principal component explains almost 15% of the variation.

3.4.3. PAO and GAO primer sets

Considering PAOs, while MiSeq coverage of the MMCs for most operational days was considered inadequate (Figs. S76 and S77), results on operational day 283 exhibited good coverage for S- and V-EBPR; similarly, for G-EBPR the coverage was sufficient on operational days 121, 241, and 283. For these operational days, all MMC were nearly 100% dominated by *Betaproteobacteria* at the class level, which was an unsurprising result given that the model PAO on which the primers are based is a *Betaproteobacteria* (He et al., 2007). At the genus level, the S-EBPR MMC was dominated by *Propionivibrio* and *Azospira* (the former at >80%); both are of the *Rhodocyclaceae* family. The V-EBPR MMC was similarly dominated by *Propionivibrio* at the genus level on operational day 283 (>80%), but *Azospira* was only 0.0034% of the MMC. The G-EBPR MMC was also enriched with *Propionivibrio* (especially on day 121 at 83.7%, which also corresponded with the best rarefaction curve of all PAO data sets). While most other data sets did not exhibit the coverage to justify significant conclusions, *Propionivibrio* nonetheless was commonly observed (in many instances dominating; Table S92). Functionally, *Propionivibrio* is a fermentative bacterium with the capability to produce short-chain VFAs (i.e., the optimal EBPR substrate) from polysaccharides (Zhou et al., 2015); given these metabolic capabilities, certain species of *Propionivibrio* could be PAOs, although recent research has identified one potential species (*Candidatus* Propionivibrio aalborgensis) as a putative GAO (Albertsen et al., 2016). Other genera including *Azonexus* and *Dechloromonas* (within the *Rhodocyclaceae* family of the *Betaproteobacteria* class) were observed, as was *Bdellovibrio* (which is within the *Bdellovibrionaceae* family of the *Deltaproteobacteria* class). The Moscow WRRF MMC was dominated by an unknown *Rhodocyclaceae* at the genus level, along with a large fraction of *Propionivibrio*. Conversely, the R-EBPR MMC was dominated by *Dechloromonas*.

Similar to the PAO MiSeq results, data obtained using the GAO primers did not exhibit sufficient coverage across all samples (Fig. S136 and S137). However, for V-EBPR on operational day 241 and for G-EBPR on days 241, 263, and 283 the coverage was sufficient to draw interpretations; additionally, the S-EBPR MMC on operational day 263 appeared to exhibit good overall coverage. The MMC were dominated by *Gammaproteobacteria*. Extrapolating to the other GAO data sets, all MMC except R-EBPR consistently showed *Gammaproteobacteria* at >86.2%.

3.5. Estimating accumulibacter and PAO relative abundance with next generation sequencing

MiSeq results were binned based on alignment, or lack thereof, with the 27 Accumulibacter sequences (He et al., 2007). To the authors' best knowledge, similar such studies on EBPR systems are few (two using *ppk* and qPCR (He et al., 2007; Mao et al., 2015); one using 454 pyrosequencing (Kim et al., 2013); one using qFISH (Albertsen et al., 2012)) and no such interrogation has been performed on MMCs in lab- or full-scale systems and across diverse wastewater substrates based on next generation sequencing data. For the Eubacterial data across all MMC, fractional Accumulibacter ranged from 0.0% to 21.45% (Table S137); while the range appears large, the second highest fraction was 4.03%. Of significance, on

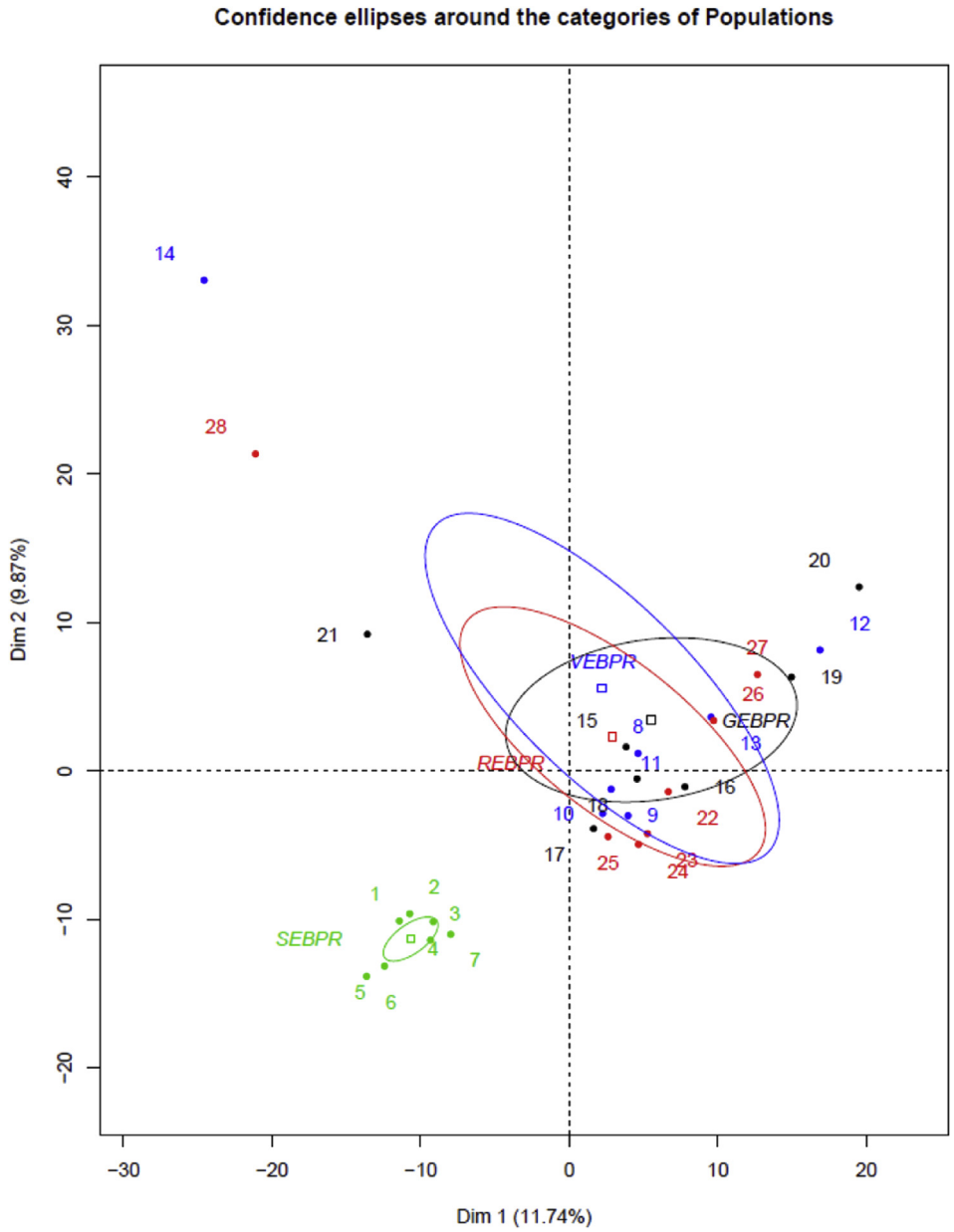

Fig. 3. Bivariate plot of the first two principal component (Dim 1 and Dim 2) scores for the 16S rRNA gene sequencing results using the EUB primer set at the genus level and the P removed. Samples have been grouped by system (distinguished by color) with the numbers corresponding to their index in an ordered list (i.e., sorted by operational day following an arbitrary system ordering: 1 to 7 are S-EBPR operational days 72–283; 8 to 14 are V-EBPR operational days 72–283; 15 to 21 are G-EBPR operational days 72–283; and 22 to 28 are R-EBPR operational days 72–283. The centroid for each group in the Dim 1-Dim 2 space is depicted as a square in the associated color and the ellipses denote the 95% confidence regions for the associated centroids in the Dim 1-Dim 2 space. (For interpretation of the references to colour in this figure legend, the reader is referred to the web version of this article.)

many operational days the data suggests no Accumulibacter were present in the MMC; in particular, the G-EBPR showed no Accumulibacter, and R-EBPR was essentially zero as well. Targeting the family *Rhodocyclaceae*, the relative abundance ranged from 0.27% to 30.38%; in contrast to the Accumulibacter results, MMC in G- and R-EBPR showed fractions comparable to that observed in V-EBPR, and higher than those observed in the Moscow WRRF. Oehmen et al. (2010) suggested that Accumulibacter fractions in real WRRFs would range from 5 to 20%; results herein suggest this range is correct for *Rhodocyclaceae* but not Accumulibacter specifically.

Comparing the qPCR and BLASTN results, no correlation was observed between the relative abundance (Eubacterial primers) for both Accumulibacter and *Rhodocyclaceae* and the qPCR data; moreover, in nearly all cases the qPCR %PAOs exceeded MiSeq estimates based on the Accumulibacter BLASTN data. Considering that all evaluated systems (with the exception of R-EBPR) performed quality P removal (Table 2), it would appear that other non-Accumulibacter species (including within the *Rhodocyclaceae* family) are PAOs, and these non-Accumulibacter species are captured (amplified) by the model PAO primers and quantified via qPCR. To the best of our knowledge, this is only the second study that interrogated real wastewater EBPR systems for PAOs using both qPCR and next generation sequencing (454 pyrosequencing or Illumina MiSeq); results of this study aligned with that of Mao et al. (2015), who similarly observed no correlation between PAOs (applying 16S rDNA and primers for *ppk*) and 454 pyrosequencing data.

3.6. Specificity of the PAO primer set

The BLASTN analysis was also carried out on the PAO primer set results to assess the specificity of the PAO primer set for both *Rhodocyclaceae* and Accumulibacter (summarized in Table S138). Unexpectedly, assignment of the sequences by RDP to *Rhodocyclaceae* was variable. Five of the seven operational days for S-EBPR had more than 96% of the sequences assigned to *Rhodocyclaceae* while none of the R-EBPR samples exceeded 88%. Alignment of the sequences with the 27 Accumulibacter sequences (He et al., 2007) was also variable. For example, S-EBPR on operational day 283 had 98.17% of the *Rhodocyclaceae* assigned sequences align with Accumulibacter, whereas G-EBPR was less than 1% on four of the seven operational days (and did not exceed 11%). As with the eubacterial primers, few to no sequences from G- and R-EBPR aligned with Accumulibacter. These results further support that the model PAO primers ultimately amplify non-Accumulibacter species (that may also be PAOs).

3.7. Identifying other potential PAOs

With the unexpected P removal performance of G-EBPR (data presented herein and in Coats et al. (2015)), coupled with the BLASTN results suggesting negligible Accumulibacter, the MiSeq data was interrogated in search of potential explanations. As described, *Propionvibrio* was dominant among the phylotypes identified with the PAO primer set at the genus level, and it may or may not be a PAO (Albertsen et al., 2016; Zhou et al., 2015). For the eubacterial primers, *Saccharibacteria* spp. was prevalent across all operational days (also present in the Moscow WRRF, but negligible in the other SBRs); these bacteria are part of the filamentous group of microorganisms referred to as TM7 (Jenkins et al., 2003). *Thiobacillus* – a *Betaproteobacteria* – was also consistently prominent in the G-EBPR MMC; this bacterium has the ability to store glycogen and could be implicated in EBPR (it was also present at 10.8% and 13.8% on average in V- and R-EBPR, respectively). Similar to *Saccharibacteria* spp., *Haliscomenobacter* (a *Bacteroidetes*) is a filamentous bacterium common to activated sludge (Jenkins et al., 2003), although it has been suggested that the bacterium cannot utilize glycerol (Kämpfer, 1995); similar enrichments were observed for this microorganism in all systems evaluated. *Zoogloea* (a *Betaproteobacteria*) are viewed as critical to floc formation in activated sludge (Wen et al., 2015), and are common in activated sludge (Liu et al., 2016); *Zoogloea* was also enriched in V- and R-EBPR. Of particular interest was the large fraction of *Defluviicoccus*, a putative GAO (Carvalheira et al., 2014). However, being an *Alphaproteobacteria*, *Defluviicoccus* is capable of PHA synthesis, and research has suggested certain clusters can store polyP (Wang et al., 2014). In fact, *Defluviicoccus* was also relatively prominent in S-EBPR and to a lesser degree in V-EBPR. Finally, *Methylobacillus* was relatively prominent in G-EBPR. *Methylobacillus* is a methanol oxidizer, but there is no known linkage to EBPR.

Regarding other bacteria potentially important to EBPR, Tu and Schuler (2013), at times, observed a relatively large fraction of *Dechloromonas* in a synthetic-fed EBPR system (and suggested the potential for associated PAO behavior). Oehmen et al. (2010) similarly suggested *Dechloromonas* might be a PAO. However, this bacterium was only present on average less than 0.72% in MMCs this study. *Azospira* (within the *Betaproteobacteria* order) was detected in S-EBPR using the PAO primers, however, this bacterium was minimally present within the eubacterial dataset, suggesting no real consequence to EBPR (or at least in systems treating real wastewater). Considering PHA production potential, and thus putative involvement with EBPR, *Thauera* (within the *Betaproteobacteria* order; a known PHA producer (Lemos et al., 2008)) was relatively prominent in S-, V-, and R-EBPR (>1% on average; Table S49), but <1% in G-EBPR and the Moscow WRRF. While *Meganema* (an *Alphaproteobacterium* capable of excess PHA synthesis (Hanson et al., 2016b)) was, on average, present in large numbers on average in V-, G-, and R-EBPR, the average was skewed due to a large fraction observed in the MMC on operational day 283.

Tetrasphaera are also linked to EBPR as putative PAOs (Nguyen et al., 2011; Nielsen et al., 2012). Being of the *Actinobacteria* phylum, the PAO primers used herein would not have amplified *Tetrasphaera*; however, the genus was identified in the Eubacterial data set. Of particular note, G-EBPR generally had the highest relative abundance of *Tetrasphaera* of the systems evaluated (Fig. 4), with values approaching parity with *Propionivibrio*. *Tetrasphaera* may be able to consume glycerol anaerobically, given the recently identified glycerol kinase in a *Tetrasphaera* species (UniProt Accession: A0A0Q9M5T8) and the genus' ability to consume glucose anaerobically (Nguyen et al., 2011). Additionally, the inability of *Tetrasphaera* to process VFAs larger than acetate (Kong et al., 2005; Nguyen et al., 2011) could explain the temporary EBPR failure observed by Coats et al. (2015) when the G-EBPR substrate was switched from crude glycerol to VFA-rich primary solids fermentate. Accordingly, *Tetrasphaera* could have contributed to the unexpected EBPR success in G-EBPR.

3.8. Relevance of PAO abundance to EBPR performance

Theory would suggest that high %PAOs within the MMC is necessary for successful EBPR; such theory is backed up by a dominant array of synthetic wastewater-based research. However, in this study attempts to relate the %PAOs with the process performance metrics proved unsuccessful. For all SBRs across all operational days, there was no apparent correlation between %PAO and effluent phosphorus or %P removal (Tables 1 and 3). Across the SBRs the highest vs. lowest observed effluent P (and associated %PAO) were 2.20 mg P L^{-1} (4.48%; S-EBPR, day 86) and 0.03 mg P L^{-1} (0.40%; V-EBPR, day 86). Moreover, the lowest observed %PAO (0.11%; R-EBPR, day 263) exhibited good P removal (76.6%). Indeed, the PAO fraction in the real wastewater lab-scale systems was estimated to be much lower than observed in the synthetic-fed SBR, yet overall P removal performance (excluding R-EBPR) was comparable. The PAO population in the full-scale EBPR system, which achieved excellent P removal, was quantitatively comparable to that of S-EBPR and consistently higher than observed in the real wastewater-based SBRs, but again no correlation could be inferred. Finally, a comparative analysis between the process metrics (VFA:P; P:C) and the qPCR PAO data revealed no correlations (data not shown). Collectively, these comparative analyses suggest that EBPR function did not follow with enrichment of PAOs. Indeed, Mao et al. (2015) and Liu et al. (2016) observed numerous full-scale systems enriched with Accumulibacter that were not operated for EBPR.

4. Conclusions

Research was conducted on lab- and full-scale EBPR systems, with a coupled examination of MMC structure (applying qPCR and Illumina MiSeq analysis) and EBPR function; investigations further considered synthetic vs. real wastewater. A central question throughout the study was the relative significance, or lack thereof, in the enrichment of a specific population of PAOs in accomplishing excess P removal. Collectively, results suggest that induced EBPR function transcends enrichment of any specific MMC population. While a strong relationship was demonstrated between EBPR metrics (P:C; influent VFA:P) and excellent P removal across diverse EBPR systems and MMCs, no such correlation existed with the specific MMCs (either based on qPCR or

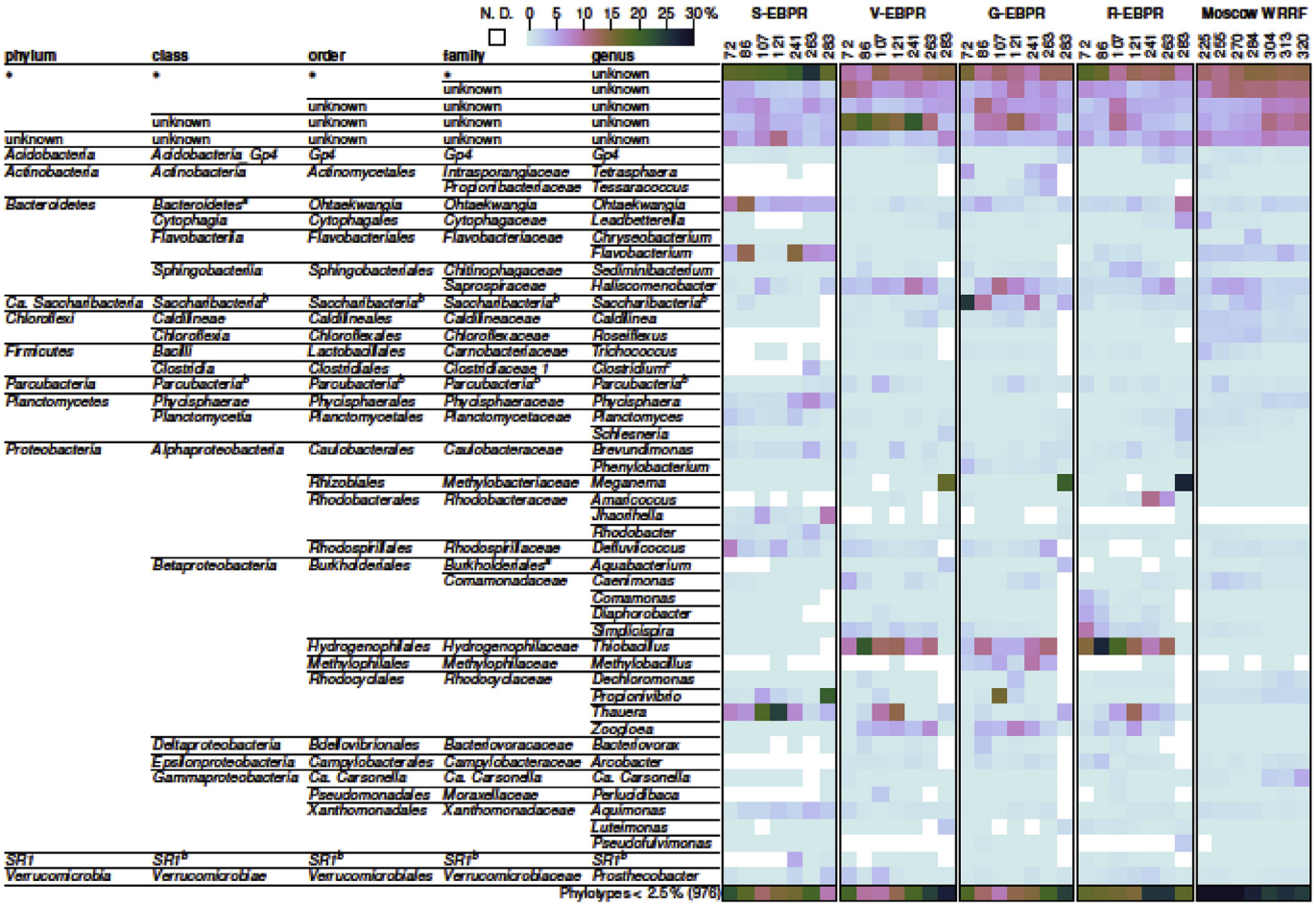

Fig. 4. Heat map showing the relative abundance of phylotypes identified at the genus level using the EUB primer set. Unidentified phylotypes (denoted as "unknown") were aggregated by the most specific taxonomic level at which they were identified (the "*" is used to indicate any identified taxon name). Note that the adopted color scheme is nonlinear at 0% relative abundance to differentiate phylotypes which were not detected (N. D.) in a sample from those that were. To conserve space, some taxon names have been abbreviated (Ca.: *Candidatus*; [a]: *_incertae_sedis*; [b]: *_genera_incertae_sedis*; and [c]: *sensu stricto*). The phylotypes with less than 2.5% relative abundance in all samples were aggregated and denoted "Phylotypes <2.5%" followed by the number of phylotypes so categorized in parentheses at the bottom of the heat map. (For interpretation of the references to colour in this figure legend, the reader is referred to the web version of this article.)

MiSeq data). Multivariate analysis of the MiSeq-described MMCs revealed distinct clusters based on substrate, with the synthetic wastewater fed MMC unique from that of the real wastewater systems, including a full-scale EBPR system. qPCR results based on primers designed for the putative PAO Accumulibacter did not correlate with BLASTN eubacterial results for either Accumulibacter or *Rhodocyclaceae*. More critically, RDP assignment of PAO-based sequences aligned poorly with Accumulibacter for both eubacterial and PAO primer sets, which strongly suggests that the conventional PAO primers applied in FISH and qPCR analysis do not sufficiently target the putative PAO Accumulibacter. In particular, negligible alignment was observed for PAO amplicons obtained from a MMC performing excellent EBPR on crude glycerol (an atypical substrate). The best observed BLASTN match of the PAO amplicons was for a synthetic wastewater-based MMC; this result raises concerns about the potential relevance in using synthetic substrates in the study of EBPR.

Acknowledgements

The material presented and discussed herein is based upon work supported by i) an Institutional Development Award (IDeA) from the National Institute of General Medical Sciences of the National Institutes of Health under Grant Number P20GM103408 and ii) the National Science Foundation under Grant Number CBET-1235885. Any opinions, findings, and conclusions or recommendations expressed in this material are those of the authors and do not necessarily reflect the views of the funding agencies.

The authors greatly appreciate the efforts of Nicholas M. Guho, who prepared and executed workflows to evaluate the MiSeq results and generate the associated tables and figures.

Appendix A. Supplementary data

Supplementary data related to this article can be found at http://dx.doi.org/10.1016/j.watres.2016.10.069.

References

Al-Najjar, M.M., Coats, E.R., Loge, F.J., 2011. The role of the microbial stringent response in excess intracellular accumulation of phosphorous in mixed consortia fed synthetic wastewater. Water Res. 45 (16), 5038–5046.

Albertsen, M., Hansen, L.B.S., Saunders, A.M., Nielsen, P.H., Nielsen, K.L., 2012. A metagenome of a full-scale microbial community carrying out enhanced biological phosphorus removal. ISME J. 6 (6), 1094–1106.

Albertsen, M., McIlroy, S.J., Stokholm-Bjerregaard, M., Karst, S.M., Nielsen, P.H., 2016. "Candidatus Propionivibrio aalborgensis": a novel glycogen accumulating organism abundant in full-scale enhanced biological phosphorus removal plants. Front. Microbiol. 7.

Bond, P.L., Hugenholtz, P., Keller, J., Blackall, L.L., 1995. Bacterial community structures of phosphate-removing and non-phosphate-removing activated sludges from sequencing batch reactors. Appl. Environ. Microb. 61 (5), 1910–1916.
Bond, P.L., Erhart, R., Wagner, M., Keller, J., Blackall, L.L., 1999. Identification of some of the major groups of bacteria in efficient and nonefficient biological phosphorus removal activated sludge systems. Appl. Environ. Microbiol. 65 (9), 4077–4084.
Brooks, B.W., Lazorchak, J.M., Howard, M.D.A., Johnson, M.-V.V., Morton, S.L., Perkins, D.A.K., Reavie, E.D., Scott, G.I., Smith, S.A., Steevens, J.A., 2016. Are harmful algal blooms becoming the greatest inland water quality threat to public health and aquatic ecosystems? Environ. Toxicol. Chem. 35 (1), 6–13.
Camacho, C., Coulouris, G., Avagyan, V., Ma, N., Papadopoulos, J., Bealer, K., Madden, T.L., 2009. BLAST+: architecture and applications. BMC Bioinform. 10 (1), 1–9.
Carvalheira, M., Oehmen, A., Carvalho, G., Reis, M.A.M., 2014. The effect of substrate competition on the metabolism of polyphosphate accumulating organisms (PAOs). Water Res. 64, 149–159.
Coats, E.R., Mockos, A., Loge, F.J., 2011a. Post-anoxic denitrification driven by PHA and glycogen within enhanced biological phosphorus removal. Bioresour. Technol. 102, 1019–1027.
Coats, E.R., Watkins, D.L., Brinkman, C.K., Loge, F.J., 2011b. Effect of anaerobic HRT on biological phosphorus removal and the enrichment of phosphorus accumulating organisms. Water Environ. Res. 83 (5), 461–469.
Coats, E.R., Watkins, D.L., Kranenburg, D., 2011c. A comprative environmental life cycle analysis for removing phosphorus from wastewater: biological versus physical/chemical processes. Water Environ. Res. 83 (8), 750–760.
Coats, E.R., Dobroth, Z.T., Brinkman, C.K., 2015. EBPR using crude glycerol: assessing process resiliency and exploring metabolic anomalies. Water Environ. Res. 87 (1), 68–79.
Crocetti, G.R., Hugenholtz, P., Bond, P.L., Schuler, A., Keller, J., Jenkins, D., Blackall, L.L., 2000. Identification of polyphosphate-accumulating organisms and design of 16S rRNA-directed probes for their detection and quantitation. Appl. Environ. Microbiol. 66 (3), 1175–1182.
Crocetti, G.R., Banfield, J.F., Keller, J., Bond, P.L., Blackall, L.L., 2002. Glycogen-accumulating organisms in laboratory-scale and full-scale wastewater treatment processes. Microbiology 148, 3353–3364.
Filipe, C.D.M., Daigger, G.T., Grady, C.P.L., 2001. Stoichiometry and kinetics of acetate uptake under anaerobic conditions by an enriched culture of phosphorus-accumulating organisms at different pHs. Biotechnol. Bioeng 76 (1), 32–43.
Garcia Martin, H., Ivanova, N., Kunin, V., Warnecke, F., Barry, K.W., McHardy, A.C., Yeates, C., He, S., Salamov, A.A., Szeto, E., Dalin, E., Putnam, N.H., Shapiro, H.J., Pangilinan, J.L., Rigoutsos, I., Kyrpides, N.C., Blackall, L.L., McMahon, K.D., Hugenholtz, P., 2006. Metagenomic analysis of two enhanced biological phosphorus removal (EBPR) sludge communities. Nat. Biotechnol. 24 (10), 1263–1269.
Grady Jr., C.P.L., Daigger, G.T., Love, N.G., Filipe, C.D.M., 2011. Biological Wastewater Treatment. IWA Publishing/CRC Press, Boca Raton, FL.
Hanson, A.J., Guho, N.M., Paszczynski, A.J., Coats, E.R., 2016a. Community proteomics provides functional insight into polyhydroxyalkanoate production by a mixed microbial culture cultivated on fermented dairy manure. Appl. Biochem. Biotechnol. 1–20.
Hanson, A.J., Paszczynski, A.J., Coats, E.R., 2016b. Proteomic profiling of an undefined microbial consortium cultured in fermented dairy manure: methods development. Electrophoresis 37 (5–6), 790–794.
He, S., Gall, D.L., McMahon, K.D., 2007. *Candidatus* Accumulibacter" population structure in enhanced biological phosphorus removal sludges as revealed by polyphosphate kinase genes. Appl. Environ. Microbiol. 73 (18), 5865–5874.
Heathwaite, L., Sharpley, A., 1999. Evaluating measures to control the impact of agricultural phosphorus on water quality. Water Sci. Technol. 39 (12), 149–155.
Hesselmann, R.P.X., Werlen, C., Hahn, D., van der Meer, J.R., Zehnder, A.J.B., 1999. Enrichment, phylogenetic analysis and detection of a bacterium that performs enhanced biological phosphate removal in activated sludge. Syst. Appl. Microbiol. 22 (3), 454–465.
Hill, T.C.J., Walsh, K.A., Harris, J.A., Moffett, B.F., 2003. Using ecological diversity measures with bacterial communities. FEMS Microbiol. Ecol. 43 (1), 1–11.
Horgan, C.J., Coats, E.R., Loge, F.J., 2010. Assessing the effects of solids residence time and volatile fatty acid augmentation on biological phosphorus removal using real wastewater. Water Environ. Res. 82 (3), 216–226.
Hu, M., Wang, X., Wen, X., Xia, Y., 2012. Microbial community structures in different wastewater treatment plants as revealed by 454-pyrosequencing analysis. Bioresour. Technol. 117, 72–79.
Jenkins, D., Richard, M.G., Daigger, G.T., 2003. Manual on the Causes and Control of Activated Sludge Bulking, Foaming, and Other Solids Separation Problems. Lewis Publishers.
Kämpfer, P., 1995. Physiological and chemotaxonomic characterization of filamentous bacteria belonging to the genus *Haliscomenobacter*. Syst. Appl. Microbiol. 18 (3), 363–367.
Kim, B.-C., Kim, S., Shin, T., Kim, H., Sang, B.-I., 2013. Comparison of the bacterial communities in anaerobic, anoxic, and oxic chambers of a pilot A2O process using pyrosequencing analysis. Curr. Microbiol. 66 (6), 555–565.
Kong, Y., Nielsen, J.L., Nielsen, P.H., 2005. Identity and ecophysiology of uncultured actinobacterial polyphosphate-accumulating organisms in full-scale enhanced biological phosphorus removal plants. Appl. Environ. Microbiol. 71 (7), 4076–4085.
Lemos, P.C., Serafim, L.S., Santos, M.M., Reis, M.A.M., Santos, H., 2003. Metabolic pathway for propionate utilization by phosphorus-accumulating organisms in activated sludge: C-13 labeling and in vivo nuclear magnetic resonance. Appl. Environ. Microb. 69 (1), 241–251.
Lemos, P.C., Levantesi, C., Serafim, L.S., Rossetti, S., Reis, M.A.M., Tandoi, V., 2008. Microbial characterisation of polyhydroxyalkanoates storing populations selected under different operating conditions using a cell-sorting RT-PCR approach. Appl. Microbiol. Biotechnol. 78 (2), 351–360.
Liu, T., Liu, S., Zheng, M., Chen, Q., Ni, J., 2016. Performance assessment of full-scale wastewater treatment plants based on seasonal variability of microbial communities via high-throughput sequencing. PLoS ONE 11 (4), e0152998.
Lopez-Vazquez, C.M., Hooijmans, C.M., Brdjanovic, D., Gijzen, H.J., van Loosdrecht, M.C.M., 2007. A practical method for quantification of phosphorus- and glycogen-accumulating organism populations in activated sludge systems. Water Environ. Res. 79 (13), 2487–2498.
Lu, H., Oehmen, A., Virdis, B., Keller, J., Yuan, Z., 2006. Obtaining highly enriched cultures of Candidatus Accumulibacter phosphates through alternating carbon sources. Water Res. 40, 3838–3848.
Magoč, T., Salzberg, S.L., 2011. FLASH: fast length adjustment of short reads to improve genome assemblies. Bioinformatics 27 (21), 2957–2963.
Mao, Y., Graham, D.W., Tamaki, H., Zhang, T., 2015. Dominant and novel clades of Candidatus Accumulibacter phosphatis in 18 globally distributed full-scale wastewater treatment plants. Sci. Rep. 5, 11857.
Muyzer, G., de Waal, E.C., Uitterlinden, A.G., 1993. Profiling of complex microbial populations by denaturing gradient gel electrophoresis analysis of polymerase chain reaction-amplified genes coding for 16S rRNA. Appl. Environ. Microbiol. 59 (3), 695–700.
Nguyen, H.T.T., Le, V.Q., Hansen, A.A., Nielsen, J.L., Nielsen, P.H., 2011. High diversity and abundance of putative polyphosphate-accumulating Tetrasphaera-related bacteria in activated sludge systems. FEMS Microbiol. Ecol. 76 (2), 256–267.
Nguyen, H.T.T., Nielsen, J.L., Nielsen, P.H., 2012. *Candidatus* Halomonas phosphatis', a novel polyphosphate-accumulating organism in full-scale enhanced biological phosphorus removal plants. Environ. Microbiol. 14 (10), 2826–2837.
Nielsen, P.H., Mielczarek, A.T., Kragelund, C., Nielsen, J.L., Saunders, A.M., Kong, Y., Hansen, A.A., Vollertsen, J., 2010. A conceptual ecosystem model of microbial communities in enhanced biological phosphorus removal plants. Water Res. 44 (17), 5070–5088.
Nielsen, P.H., Saunders, A.M., Hansen, A.A., Larsen, P., Nielsen, J.L., 2012. Microbial communities involved in enhanced biological phosphorus removal from wastewater — a model system in environmental biotechnology. Curr. Opin. Biotechnol. 23 (3), 452–459.
Oehmen, A., Lemos, P.C., Carvalho, G., Yuan, Z.G., Keller, J., Blackall, L.L., Reis, M.A.M., 2007. Advances in enhanced biological phosphorus removal: from micro to macro scale. Water Res. 41 (11), 2271–2300.
Oehmen, A., Carvalho, G., Lopez-Vazquez, C.M., van Loosdrecht, M.C.M., Reis, M.A.M., 2010. Incorporating microbial ecology into the metabolic modelling of polyphosphate accumulating organisms and glycogen accumulating organisms. Water Res. 44, 4992–5004.
Paerl, H., 2014. Mitigating harmful cyanobacterial blooms in a human- and climatically-impacted world. Life 4 (4), 988.
Pretty, J.N., Mason, C.F., Nedwell, D.B., Hine, R.E., Leak, S., Dils, R., 2003. Environmental costs of freshwater eutrophication in England and Wales. Environ. Sci. Technol. 37 (2), 201–208.
Ramakers, C., Ruijter, J.M., Deprez, R.H.L., Moorman, A.F.M., 2003. Assumption-free analysis of quantitative real-time polymerase chain reaction (PCR) data. Neurosci. Lett. 339 (1), 62–66.
Seviour, R.J., Mino, T., Onuki, M., 2003. The microbiology of biological phosphorus removal in activated sludge systems. FEMS Microbiol. Rev. 27, 99–127.
Shen, J., Song, N., Williams, C.J., Brown, C.J., Yan, Z., Xu, C., Forney, L.J., 2016. Effects of low dose estrogen therapy on the vaginal microbiomes of women with atrophic vaginitis. Sci. Rep. 6, 24380.
Smolders, G.J.F., van der Meij, J., van Loosdrecht, M.C.M., Heijnen, J.J., 1994. Model of the anaerobic metabolism of the biological phosphorus removal process: stoichiometry and pH influence. Biotechnol. Bioeng. 43 (6), 461–470.
Thompson, J.C., He, B.B., 2006. Characterization of crude glycerol from biodiesel production from multiple feedstocks. Appl. Eng. Agric. 22 (2), 261–265.
Tu, Y., Schuler, A.J., 2013. Low acetate concentrations favor polyphosphate-accumulating organisms over glycogen-accumulating organisms in enhanced biological phosphorus removal from wastewater. Environ. Sci. Technol. 47 (8), 3816–3824.
Wang, Q., Garrity, G.M., Tiedje, J.M., Cole, J.R., 2007. Naïve Bayesian classifier for rapid assignment of rRNA sequences into the new bacterial taxonomy. Appl. Environ. Microbiol. 73 (16), 5261–5267.
Wang, X., Hu, M., Xia, Y., Wen, X., Ding, K., 2012. Pyrosequencing analysis of bacterial diversity in 14 wastewater treatment systems in China. Appl. Environ. Microb. 78 (19), 7042–7047.
Wang, Z., Guo, F., Mao, Y., Xia, Y., Zhang, T., 2014. Metabolic characteristics of a glycogen-accumulating organism in *Defluviicoccus* cluster ii revealed by comparative genomics. Microb. Ecol. 68 (4), 716–728.
WEF, 2010. Nutrient Removal: Manual of Practice No. 34. WEF Press, Alexandria, Virginia.
Wen, Y., Jin, Y., Wang, J., Cai, L., 2015. MiSeq sequencing analysis of bacterial community structures in wastewater treatment plants. Pol. J. Environ. Stud. 24 (4), 1809–1815.
Winkler, M., Coats, E.R., Brinkman, C.K., 2011. Advancing post-anoxic denitrification for biological nutrient removal. Water Res. 45 (18), 6119–6130.

Zhang, H., Sekiguchi, Y., Hanada, S., Hugenholtz, P., Kim, H., Kamagata, Y., Nakamura, K., 2003. *Gemmatimonas aurantiaca* gen. nov., sp. nov., a Gram-negative, aerobic, polyphosphate-accumulating micro-organism, the first cultured representative of the new bacterial phylum *Gemmatimonadetes* phyl. nov. Int. J. Syst. Evol. Microbiol. 53 (4), 1155–1163.

Zhou, Z., Qiao, W., Xing, C., An, Y., Shen, X., Ren, W., Jiang, L.-m., Wang, L., 2015. Microbial community structure of anoxic–oxic-settling-anaerobic sludge reduction process revealed by 454-pyrosequencing. Chem. Eng. J. 266, 249–257.